Geophys. J. Int. (1999) **138,** 702–716

Path-summation waveforms

Anthony Lomax

Géosciences-Azur, Universtiy of Nice—Sophia Antipolis, 250 *Rue Albert Einstein,* 06560 *Valbonne, France. E-mail: lomax@faille.unice.fr*

Accepted 1999 April 1. Received 1999 February 11; in original form 1998 May 18

SUMMARY

In this paper, we examine an efficient, practical method to calculate approximate, finite-frequency waveforms for the early signals from a point source in 3-D acoustic media with smoothly varying velocity and constant density. In analogy to the use of Feynman path integrals in quantum physics, we obtain an approximate waveform solution for the scalar wave equation by a Monte Carlo summation of elementary signals over a representative sample of all possible paths between a source and observation point. The elementary signal is formed from the convolution of the source time function with a time derivative of the Green's function for the homogeneous problem. For each path, this elementary signal is summed into a time series at a traveltime obtained from an integral of slowness along the path. The constructive and destructive interference of these signals produces the approximate waveform response for the range of traveltimes covered by the sampled paths.

We justify the path-summation technique for a smooth medium using a heuristic construction involving the Helmholtz–Kirchhoff integral theorem. The technique can be applied to smooth, but strongly varying and complicated velocity structures. The approximate waveform includes geometrical spreading, focusing, defocusing and phase changes, but does not fully account for multiple scattering. We compare path-summation waveforms with the exact solution for a 3-D geometry involving a low-velocity spherical inclusion, and with finite-difference waveforms for a 2-D structure with realistic, complicated velocity variations.

In contrast to geometrical-ray methods, the path-summation approach reproduces finite-frequency wave phenomena such as diffraction and does not exhibit singular behaviour. Relative to the finite-difference numerical method, the path-summation approach requires insignificant computer memory and, depending on the number of waveforms required, up to one to two orders of magnitude less computing time. The sampled paths and associated traveltimes produced by the path summation give a relation between the medium and the signal on the waveform that is not available with finite-difference and finite-element methods. Furthermore, the speed and accuracy of the path-summation method may be sufficient to allow 3-D waveform inversion using stochastic, non-linear, global search methods.

Key words: inversion, lateral heterogeneity, synthetic waveforms, wave equation, wave propagation.

INTRODUCTION

It is important to have computationally efficient methods for modelling finite-frequency or broad-band wave propagation in structures with strong velocity variations in three dimensions. Such methods may allow non-linear inversion of waveform data for problems in fields such as seismology and ocean acoustics, where complicated velocity structures or wavefields are expected. This inversion would make use of much more of the information contained in high-quality waveform data sets than do existing techniques such as first arrival time inversion.

Existing methods for modelling scalar, acoustic or elastic wave propagation are variations on three, basic, complementary approaches—ray, frequency–wavenumber summation, and numerical calculations such as finite differences and finite elements. Ray-based techniques are efficient and can be used with complicated media, but are valid only if the wavelengths involved are much smaller than any characteristic length in

the medium, or, equivalently, these techniques are valid only at very high frequencies. These methods cannot produce finite-frequency phenomena such as diffraction and head waves, and they fail at singular regions of the finite-frequency wavefield, for example near caustics. However, there are many formal and ad-hoc extensions to ray theory that recover some of these phenomena in the high-frequency limit. In contrast to ray-based methods, frequency–wavenumber of modal-summation techniques are valid for a broad range of frequencies and can produce exact waveforms, but these methods are only applicable for relatively simple and highly symmetric structures. Finally, numerically intensive techniques such as finite elements and finite differences can accurately model full wave phenomena in complicated structures, but these methods typically require large to very large computing resources and computing time. Other hybrid techniques, such as Kirchhoff–Helmholtz–Fresnel and related boundary-integral methods, may combine features and advantages from the three basic approaches, but they also retain some of the disadvantages and limitations.

In this paper, we introduce an efficient 'path-summation' technique to obtain approximate waveforms due to finite-frequency, scalar wave propagation from a point source with arbitrary source time function in media with smooth, 3-D velocity variations. These waveforms are approximate solutions to the scalar wave equation; this equation represents the acoustic case with constant density. The path-summation method combines many of the advantages of the three basic, existing approaches, and it may be fast and accurate enough to allow imaging of complicated 3-D structures through non-linear inversion of waveforms.

The path-summation method constructs an approximate solution to the scalar wave equation by Monte Carlo summation over the contributions of elementary signals 'propagated' along a representative sample of all possible paths between the source and observation points (Fig. 1a). The elementary signal is given by the convolution of the source time function with a time derivative of the Green's function for the homogeneous problem. This elementary signal is summed into a waveform at an offset time given by a *traveltime* (integral of slowness) along each path. The amplitude of the resulting waveform is scaled by a factor that depends on the distance of the observation point from the source, the number of paths used, and other quantities. The constructive and destructive interference of the elementary signals contributed by each path produces a waveform that converges towards the approximate response for the portion of the medium and range of traveltimes covered by the sampled paths. For example, the constructive interference of elementary signals from a large number of paths with nearly identical traveltimes will produce prominent features on the waveform. In contrast, the interference of signals from many paths with well-distributed traveltimes will converge to a flat trace. This procedure for obtaining a solution to the scalar wave equation forms an analogue to the Feynman path-integral technique (Feynman 1948; Feynman & Hibbs 1965; Feynman 1985; Weigel 1986), a basic tool in elementary particle physics for the study and understanding of quantum phenomena.

In practice, the approximate nature of the 'path-summation' technique and computational limitations will impose upper bounds on the model complexity, maximum frequency and source–receiver distances that can be studied. In a 2-D example, we will see that this method can be applied to smooth media

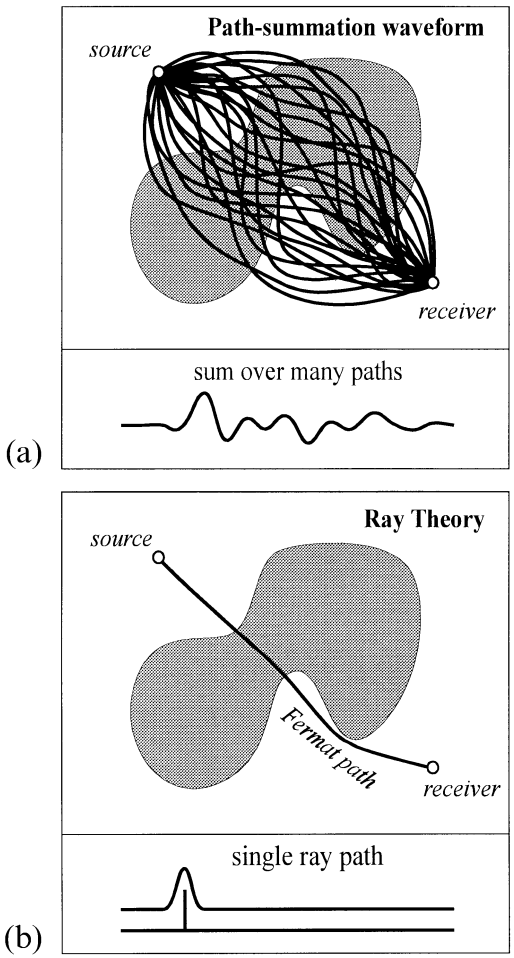

Figure 1. (a) Schematic illustration of the path-summation waveform method; this method samples many paths that fill a volume of the medium. (b) Schematic illustration of a ray-based method; ray methods sample the medium only along one or a few paths.

with velocity variations the size of and larger than the dominant wavelength of the source signal, to obtain the first-arriving waveforms at distances of about 10 times the dominant wavelength.

We begin by reviewing the path-integral concept in physics, and then we present a heuristic development using the Helmholtz–Kirchhoff integral theorem to arrive at an approximate, path-summation solution for the scalar wave equation in three dimensions. Next, we examine the performance of this path-summation waveform method relative to an exact solution for a 3-D problem involving a low-velocity sphere embedded in a homogeneous whole-space. We then compare the waveforms from a 2-D form of the path-summation formula with waveforms from finite differences for a realistic 2-D medium. Finally, we use the 2-D path-summation results to examine the relationships between the sampled paths and features of the waveforms and the model.

FEYNMAN PATH INTEGRALS

In 1948, Richard Feynman introduced the path-integral method as a new formulation of non-relativistic quantum mechanics and showed that this formulation satisfies the Schrödinger

equation (Feynman 1948). Since this time, 'Feynman' path integrals have been fruitfully applied in physics and other physical sciences to a diverse range of problems (e.g. Schulman 1988; Wiegel 1986; Khandekar *et al.* 1993).

The path-integral method as presented by Feynman (1948) states that the probability that an event occurs is given by the square of the sum of complex amplitude contributions from all possible ways that the event could occur. For problems in quantum physics, these 'ways' are space–time paths between two states of a particle. For a quantum particle, the contribution from each path is equal in magnitude but varies in phase according to the 'action' of classical physics, that is the time integral of the Lagrangian of the system as the particle follows the spacetime path (Feynman 1948). There are thus contributions to the amplitude sum not just from 'classical' paths of minimum 'action', but also from an infinite number of 'non-classical' paths. The resulting expression for the probability includes both familiar, 'classical' phenomena and unusual, qualitatively different, quantum mechanical behaviour.

The quantum behaviour arises from the constructive and destructive interference of the complex amplitude values in the path-integral sum. The use of complex amplitudes is related to the 'wave-like' behaviour of quantum 'particles'. As a consequence, we find parallels between the classical–quantum duality in particle physics and the ray–wave duality in optics or elasticity. This is underlined by an example that Feynman uses to illustrate the path-integral concept. He shows (Feynman 1985) that a consideration of the traveltime (or phase delay) along all possible paths that light could take between two points predicts the well-known geometrical-optics result that light 'follows' the path of least time—the Fermat path. However, additionally, he shows that this multiple-path approach also produces diffraction, a non-geometrical result. We see in this simple optics example that the path-integral approach does not rely on the representation of light as travelling along one or a few, infinitesimally narrow rays. Instead it represents the light as sampling a large volume between the two points (*cf.* the paths in Figs 1a and b). Consequently, many paths other than Fermat paths are considered, and non-geometrical, finite-frequency phenomena are obtained.

In the physical sciences, the Feynman path integral is invoked for problems where the wave equation can be transformed to a parabolic equation with the form of the Schrödinger equation (e.g. Dashen 1979; Klauder 1986; Patton 1986; Ziolkowski 1986). These formulations are valid only for high-frequency waves and for media in which properties vary predominantly along one spatial dimension, but they allow the stable analysis of phenomena for which geometrical optics fails, such as diffraction and propagation near caustics. These high-frequency solutions are related to the WKBJ approximation (Schulman 1981). Path-integral solutions for the scalar wave equation can also be obtained by introducing a 'pseudo-time' variable that is used to transform the frequency-domain equation to a parabolic form (e.g. Fishman & McCoy 1983; Samelsohn & Mazar 1996). However, these solutions require integration over the 'pseudo-time' variable and over frequency, in addition to the integral over paths, and consequently it is not apparent that they can be efficiently evaluated in practice for heterogeneous media. Following this 'pseudo-time' approach, Schlottmann (1999) has succeeded in evaluating the integrals analytically over the 'pseudo-time' variable and frequency to obtain a time-domain, path-integral solution for the full acoustic equation, including variable density. This solution includes a sum over all time derivatives of the source time function; Schlottmann (1999) proposes that this sum is necessary to account for all multiple scattering in heterogeneous media. It will be important to see if this solution can be efficiently evaluated in practice for heterogeneous media, as it may then form a more accurate and complete alternative to the approximate path-summation method we examine in this paper.

Finally, in astrophysics, Williamson (1975) uses a 'stochastic ray' method that is related to path integrals to study small-angle, multiple-path scattering of electromagnetic radiation passing through planar scattering regions of the interstellar medium. This method constructs the approximate response at an observation point using a Monte-Carlo summation over scattered 'elemental pulses' that have been delayed in time relative to the direct radiation because of the increased length of their paths. This methodology is qualitatively similar to the path-summation waveform technique that we present here.

In summary, it appears that a path-integral-type solution for finite-frequency, scalar wave propagation in heterogeneous media does not yet exist in a form that can be implemented in practice. As an alternative, following the path-integral concept, we develop below an approximate, path-summation solution for the scalar wave equation. We will see that this solution can be applied in practice and that it gives promising results in heterogeneous media.

HEURISTIC DEVELOPMENT OF AN APPROXIMATE, PATH-SUMMATION SOLUTION FOR THE SCALAR WAVE EQUATION

The scalar wave equation for field $\psi(\mathbf{r}, t)$ can be expressed as

$$\nabla^2\psi(\mathbf{r}, t) - \frac{1}{c^2(\mathbf{r})}\frac{\partial^2\psi(\mathbf{r}, t)}{\partial t^2} = 0, \qquad (1)$$

where t is time and the quantity $c(\mathbf{r})$ is a function of position $\mathbf{r}$ (e.g. Morse & Feshbach 1953; Tolstoy 1973). $c(\mathbf{r})$ has the units of velocity and may be referred to as a 'structural' or 'medium' velocity, but it does not specify a wave velocity except for infinite-frequency waves, or for plane waves if $c(\mathbf{r})$ is constant (Wieland 1993). For the study of sound, the scalar wave equation follows from the acoustic equation of motion for the case of constant density and spatially varying compressibility. The scalar wave equation also specifies the approximate behaviour of the potentials for longitudinal or transverse waves in smoothly varying elastic media when conversions between the two wave types can be neglected.

In the following we invoke a heuristic development involving the Helmholtz–Kirchhoff integral theorem and several simplifications valid for smooth media, to obtain an approximate, path-summation solution of the scalar wave. However, the resulting formula is an infinite sum, which cannot be evaluated in practice. We obtain normalization terms and a rule for path selection for a practical, finite-sum solution by demanding that this solution give the correct response for a homogeneous medium. Finally, we propose that this finite, path-summation formula also forms an approximate solution of the scalar wave equation for a medium with heterogeneous velocity $c(\mathbf{r})$.

The Helmholtz–Kirchhoff integral

The Helmholtz–Kirchhoff integral is a formal mathematical expression of the Huygens–Fresnel principle, which states that the field on a wavefront is given by the sum over secondary wavelets emitted at every point of the wavefront at an earlier time.

We first obtain Helmholtz–Kirchhoff integral for an inhomogeneous medium. We consider a wave field $\psi(\mathbf{r}, t)$ which satisfies the scalar wave equation (1), and the Green's function $g(\mathbf{r}, t; \mathbf{r}_0, t_0)$ for the scalar wave equation with an impulsive source term,

$$\nabla^2 g(\mathbf{r}, t; \mathbf{r}_0, t_0) - \frac{1}{c^2(\mathbf{r})} \frac{\partial^2 g(\mathbf{r}, t; \mathbf{r}_0, t_0)}{\partial t^2} = -4\pi\delta(\mathbf{r} - \mathbf{r}_0)\delta(t - t_0). \tag{2}$$

Green's theorem states that

$$\iiint_V (\phi_1 \nabla^2 \phi_2 - \phi_2 \nabla^2 \phi_1)\, dV = \iint_S \left(\phi_1 \frac{\partial \phi_2}{\partial n} - \phi_2 \frac{\partial \phi_1}{\partial n} \right) dS, \tag{3}$$

where V is a volume bounded by the closed surface S; ϕ_1 and ϕ_2 are functions with continuous first and second derivatives within V and on S; and ∂/∂_n denotes differentiation along the normal vector on S. We substitute $\psi(\mathbf{r}, t)$ and $g(\mathbf{r}, t; \mathbf{r}_S, t_S)$ for ϕ_1 and ϕ_2, with $\mathbf{r}$ inside S, and initial values $\psi(\mathbf{r}, t_S = 0) = 0$ and $(\partial/\partial t)\psi(\mathbf{r}, t_S = 0) = 0$, where the subscript S denotes quantities evaluated on the surface S. It can then be shown that Green's theorem (3) reduces to an compact expression for $\psi(\mathbf{r}, t)$:

$$\psi(\mathbf{r}, t) = \frac{1}{4\pi} \int_0^\infty dt_S \iint_S \left\{ \psi(\mathbf{r}_S, t_S) \frac{\partial}{\partial n} g(\mathbf{r}, t; \mathbf{r}_S, t_S) - g(\mathbf{r}, t; \mathbf{r}_S, t_S) \frac{\partial}{\partial n} \psi(\mathbf{r}_S, t_S) \right\} dS. \tag{4}$$

(e.g. Scott & Helmberger 1983; Frazer & Sinton 1984; Carter & Frazer 1984; or, for the homogeneous case, Morse & Feshbach 1953; Born & Wolf 1980). This form of the Helmholtz–Kirchhoff theorem expresses the field $\psi(\mathbf{r}, t)$ in terms of an integral of ψ and g and their derivatives over the surface S at the 'retarded' time t_S.

An approximate path-summation solution

We now obtain an approximate, path-summation expression for the Green's function response due to an impulsive source $4\pi\delta(t - t_0)\delta(\mathbf{r} - \mathbf{r}_0)$ in a medium with velocity $c = c(\mathbf{r})$. We follow a heuristic development beginning with a construction based on repeated, local application of the Helmholtz–Kirchhoff integral (4).

We consider a small sphere S_1 of radius r, centred on the observation point $\mathbf{r}$ (Fig. 2). We obtain the Green's function $g_{\mathrm{PS}}(\mathbf{r}, t; \mathbf{r}_0, t_0)$ by applying the integral (4) on the surface of S_1. We perform this integration by summing over the contributions of the field on N surface elements $dS_{1,n}$, in the limit $N \to \infty$; $dS_{1,n} \to 0$. Similarly, we can obtain the field on each surface element $dS_{1,n}$ on S_1 by again applying the integral (4) using additional small spheres S_{1n} centred on each $dS_{1,n}$. For each new sphere S_{1n}, we sum over the contributions of the field on M surface elements $dS_{1n,m}$, in the limit $M \to \infty$; $dS_{1n,m} \to 0$.

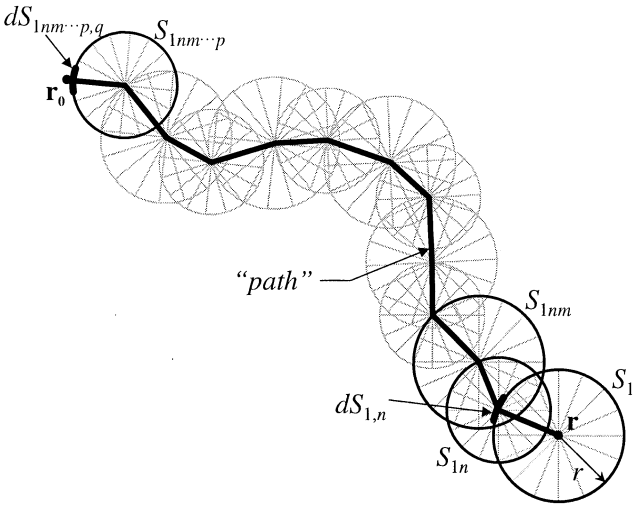

Figure 2. The recursive construction used to obtain the signal at observation point $\mathbf{r}$ due to an impulsive source at $\mathbf{r}_0$ in a heterogeneous medium. The Helmholtz–Kirchhoff integral is evaluated sequentially on a large number of small spherical surfaces; this evaluation can be re-arranged as a sum over paths. Only the spherical surfaces corresponding to one path are shown. See the text for details.

Continuing this process for each surface element on each new sphere, we obtain a tree-structure calculation involving a very large number of spherical surfaces on which we evaluate the Helmholtz–Kirchhoff integral. The evaluation of these integrals begins at surface elements $dS_{1nm\ldots p,q}$ that are infinitesimally close to the source at $\mathbf{r}_0$, and continues back towards the root spheres S_1 at the observation point $\mathbf{r}$ (Fig. 2). Expressed mathematically, this calculation has the form of a set of nested, infinite sums,

$$g_{\mathrm{PS}}(\mathbf{r}, t; \mathbf{r}_0, t_0) \approx \lim_{N,M,\ldots,Q \to \infty} \sum_{n=1}^{N} dS_{1,n} \times L\left\{ \sum_{m=1}^{M} dS_{1n,m} L\left\{ \ldots \sum_{q=1}^{Q} dS_{1nm\ldots p,q} L\{d\psi_0\} \right\} \right\}, \tag{5}$$

where $d\psi_0$ is an 'elementary' contribution of the source at each surface element $dS_{1nm\ldots p,q}$ that comes infinitesimally close to the source, and $L\{\psi\}$ is the operator forming the integrand of the Helmholtz–Kirchhoff integral (4),

$$L\{\psi\} = \frac{1}{4\pi} \int_0^\infty dt_S \left(\psi \frac{\partial}{\partial n} g - g \frac{\partial}{\partial n} \psi \right). \tag{6}$$

We now make the important assumptions that the nested infinite sum (5) is mathematically meaningful and that it is convergent; we leave further discussion and proof of these assumptions for future work.

Now, because $L\{\psi\}$ is linear in ψ, the nested sum (5) can be rearranged into an infinite sum over 'paths' from $\mathbf{r}_0$ to $\mathbf{r}$ (Fig. 2), where each path passes through one surface element on a suite of spheres $S_1, S_{1n}, \ldots S_{1nm\ldots p}$:

$$g_{\mathrm{PS}}(\mathbf{r}, t; \mathbf{r}_0, t_0) \approx \lim_{N,M,\ldots,Q \to \infty} \sum_{n=1}^{N} \sum_{m=1}^{M} \ldots \sum_{q=1}^{Q} dS_{1,n} \times L\{dS_{1n,m} L\{\ldots dS_{1nm\ldots p,q} L\{d\psi_0\}\}\}. \tag{7}$$

This rearrangement will allow us ultimately to obtain an estimate for the response $g_{PS}(\mathbf{r}, t; \mathbf{r}_0, t_0)$ by summing over a representative sample of all possible paths from $\mathbf{r}_0$ to $\mathbf{r}$. The expression (7), however, cannot be evaluated in practice. Consequently, assuming a smooth medium, we next develop approximations for $d\psi_0$ and $L\{\psi\}$ such that the infinite sum over 'paths' (7) collapses to a simple, usable form. For conciseness, but without loss of generality, we use $t_0 = 0$ in the remainder of this section.

Smooth, heterogeneous medium

We first obtain an expression for the 'elementary' source contribution $d\psi_0$ in (7) by examining the Green's function response infinitesimally close to the source. Assuming a smooth medium, we can take a small region around the source at $\mathbf{r} = \mathbf{r}_0$ as homogeneous, with constant velocity $c_0 = c(\mathbf{r}_0)$. We thus associate the contribution $d\psi_0$ with the Green's function response for the homogeneous case $g_H(\mathbf{r}, t; \mathbf{r}_0, 0)$ in the limit $\mathbf{r} \to \mathbf{r}_0$:

$$\lim_{\mathbf{r}\to\mathbf{r}_0} g_H(\mathbf{r}, t; \mathbf{r}_0, 0) = \lim_{r\to 0} \frac{\delta(t - r/c_0)}{r}. \tag{8}$$

Substituting $\xi = r/c_0$, the right side of (8) becomes

$$\lim_{\xi\to 0} \frac{\delta(t-\xi)}{c_0 \xi}, \tag{9}$$

which, by symmetry of the terms t and ξ inside the delta function, is equivalent to

$$\lim_{\xi\to 0} -\frac{\delta(t-\xi)}{c_0 t} = -\frac{\delta(t)}{c_0 t}. \tag{10}$$

Now, we use the identity $\delta'(t) = -\delta(t)/t$ to arrive at

$$\lim_{\mathbf{r}\to\mathbf{r}_0} g_H(\mathbf{r}, t) = \frac{\delta'(t)}{c_0}. \tag{11}$$

Returning to our smooth, heterogeneous medium, and replacing c_0 with the velocity at the source, $c(\mathbf{r}_0)$, expression (11) indicates that we can take

$$d\psi_0 = \frac{\delta'(t)}{c(\mathbf{r}_0)}, \tag{12}$$

as the 'elementary' contribution of the source to each path.

Next, to obtain a concise approximation for the operator $L\{\psi\}$ in the sum (7), we again assume a smooth velocity variation and, following Carter & Frazer (1984), we put

$$g(\mathbf{r}, t; \mathbf{r}_S, t_S) \cong G(\mathbf{r})\delta(t - t_S - \tau), \tag{13}$$

where $G(\mathbf{r})$ is an amplitude term and τ is the geometrical optics traveltime from $\mathbf{r}_0$ to $\mathbf{r}$. In addition, because we use small spheres S in constructing our infinite sum over paths (7), we need only 'propagate' our Green's function (13) over vanishingly small distances relative to any length-scale of velocity variation. This suggests approximating the Green's function with an expanding, spherical wave. To this end, we take a simple form for the amplitude term $G(\mathbf{r})$ that partly accounts for smooth velocity variation in the medium:

$$G(\mathbf{r}) = \frac{1}{s}\sqrt{\frac{c(\mathbf{r}_s)}{c(\mathbf{r})}}, \tag{14}$$

where $s = |\mathbf{r} - \mathbf{r}_s|$. This expression reduces to the expected $1/s$ geometrical spreading function in the homogeneous case, while for a heterogeneous medium it is scaled by the square-root term that accounts for the conservation of energy within any solid angle $d\Omega$ on the spreading wavefront; that is,

$$\rho c(\mathbf{r}) s^2 d\Omega |G(\mathbf{r})|^2 = \text{constant}, \tag{15}$$

where ρ is the constant density of the medium.

Substituting (13) and (14) into (4), neglecting derivatives of the velocity, evaluating the integral over time, and dropping the subscripts S, we obtain

$$\psi(\mathbf{r}, t) \approx \frac{1}{4\pi} \times \int\!\!\int_S \sqrt{\frac{c(\mathbf{r}_s)}{c(\mathbf{r})}} \left\{ [\psi] \frac{\partial}{\partial n}\left(\frac{1}{s}\right) - \frac{1}{c(\mathbf{r})}\frac{1}{s}\frac{\partial s}{\partial n}\left[\frac{\partial \psi}{\partial t}\right] - \frac{1}{s}\left[\frac{\partial \psi}{\partial n}\right]\right\} dS, \tag{16}$$

where s is distance along the geometrical optics ray path from $\mathbf{r}_s$ to $\mathbf{r}$. This is an approximate form of the Helmholtz–Kirchhoff integral (4) for surfaces S enclosing small volumes in a smooth, heterogeneous medium. The normal to S is taken positive *inwards* and square brackets denote values of the functions taken at the 'retarded' time $t_S = t - s/c$.

Now with the form of the integrand $L\{\psi\}$ given in (16) we can examine the 'propagation' of the elementary contribution of the source $d\psi_0$, expression (12), along a path in the sum (7). We note that along any path all of the square-root amplitude terms collapse to the single factor $\sqrt{c(\mathbf{r}_0)/c(\mathbf{r})}$; for conciseness we do not include this term in the following. We will show by induction that the elementary contribution at point P_j on the path can be approximated by

$$d\psi_j \approx \frac{1}{N^j c_0}\delta'(t - \tau_j), \tag{17}$$

where $\tau_j = \tau_{j-1} + r_j/c_j$ is the traveltime or integral over slowness along the path from the source point P_0 to point P_j, r_j is the distance along the path between points P_j and P_{j-1}, c_j is the velocity at point P_j, and $c_0 = c(\mathbf{r}_0)$ (Fig. 2). For simplicity of notation, but without loss of generality, we have taken the same radius and number N of surface elements of area dS for each sphere.

Clearly, if we consider the source point, where $j = 0$ and $\tau_0 = 0$, expression (17) evaluates to that for the elementary contribution at the source (12). Next, considering an arbitrary point P_j along the path, we assume that the elementary contribution $d\psi_j$ at P_j is given by (17), and then seek to confirm that this expression is valid for the contribution $d\psi_{j+1}$ at point P_{j+1}. Substituting r_{j+1} for s and c_{j+1} for $c(\mathbf{r})$ in (16), the elementary contribution $d\psi_{j+1}$ at point P_{j+1}, evaluated at the retarded time $t - r_{j+1}/c_{j+1}$, is

$$d\psi_{j+1} = dS\frac{1}{4\pi}L\{d\psi_j\} = \frac{4\pi r_{j+1}^2}{N}\frac{1}{4\pi}L\{d\psi_j\} = \frac{1}{N^{j+1}c_0}\left\{\delta'(t-\tau_{j+1}) + \frac{r_{j+1}}{c_{j+1}}\delta''(t-\tau_{j+1}) - r_{j+1}\cos\theta\left(\frac{1}{c_j} - \frac{r_j}{c_j^2}\frac{\partial c}{\partial r}\bigg|_{P_j}\right)\delta''(t-\tau_{j+1})\right\}, \tag{18}$$

where θ is the angle of change of direction of the path at P_j. Now we take the distance between points to be arbitrarily

small; that is, $r_i = \varepsilon_i \ll 1$. This is consistent with our previous requirement that the spheres in our recursive application of the Helmholtz–Kirchhoff integral should be very small. This, and the fact that in a smooth medium $\partial c/\partial r|_{P_j}$ is bounded, suggests that we may neglect terms in r_j and r_{j+1}. If we neglect these terms, then (18) simplifies to

$$d\psi_{j+1} \approx \frac{1}{N^{j+1} c_0} \delta'(t - \tau_{j+1}). \tag{19}$$

This expression is the same as (17), with index $j+1$ replacing j. Thus we have shown that (17) is valid at the source point and between two consecutive points along a path, and so, by induction, it is valid at all points along a path starting at the source.

Comparing expressions (17) and (19), we note that $d\psi_{j+1}$ differs from $d\psi_j$ only by a change in traveltime from τ_j to $\tau_{j+1} = \tau_j + r_{j+1}/c_{j+1}$, and by a factor $1/N$. Thus, in lieu of evaluating all of the nested operators in the sum (7), we need only calculate the traveltime along each path, and apply an appropriate normalization. The simplicity of this result will allow in part for the practical evaluation of our final path-summation formula.

Finally, writing the nested sum (7) as a single sum over $K \to \infty$ paths for $\mathbf{r}_0$ to $\mathbf{r}$, where $K = NM \ldots Q$, and substituting the results (12) and (17), we obtain an estimate for the impulse response $g_{\mathrm{PS}}(\mathbf{r}, t; \mathbf{r}_0, t_0)$:

$$g_{\mathrm{PS}}(\mathbf{r}, t; \mathbf{r}_0, t_0 = 0) \approx \lim_{\substack{K\to\infty \\ N\to\infty}} \frac{1}{\sqrt{c(\mathbf{r}_0)c(\mathbf{r})}} \sum_{k=1}^{K} \frac{1}{N^{p_k}} \delta'(t - T_k), \tag{20}$$

where $p_k = p_k(N, k)$ is the number of small spheres or segments along path k, and

$$T_k = \int_{\mathbf{r}_0}^{\mathbf{r}} \frac{ds_k}{c(\mathbf{r})} \tag{21}$$

is the integrated slowness, or traveltime, along path k. We note that the path geometry and the normalization term $1/N^{p_k}$ in the sum (20) are independent of the velocity variation $c(\mathbf{r})$.

In practice, the infinite sum (20) must be evaluated using a finite sample of paths. Thus we need rules for choosing an appropriate finite sample of paths and we need the corresponding normalization terms for these paths, in lieu of the term $1/N^{p_k}$ in (20). In the next section we use the known solution for a point source in a homogeneous medium to obtain normalization terms and a rule for path selection that allow for a practical evaluation of the sum (20).

A practical path-summation formulation

We develop a practical path-summation formula for a finite sample of paths by assuming that we can replace the term $1/N^{p_k}$ in the sum (20) with a factor A independent of the path k. We then find A and a rule for path selection such that the resulting expression $\tilde{g}^{\text{3-D}}_{\mathrm{PS,H}}$ reproduces the correct Green's function response for the homogeneous case with velocity c,

$$g^{\text{3-D}}_{\mathrm{H}}(\mathbf{r}, t; \mathbf{r}_0, 0) = \frac{\delta(t - r/c)}{r}. \tag{22}$$

Substituting a factor A outside the sum for the term $1/N^{p_k}$ in (20), we have

$$\tilde{g}^{\text{3-D}}_{\mathrm{PS,H}} = \lim_{K\to\infty} \frac{A}{c} \sum_{k=1}^{K} \delta'(t - T_k), \tag{23}$$

where $T_k = \rho_k/c$ and ρ_k is the length of the kth path. If we now require that the path lengths ρ_k are uniformly distributed between the minimum length r and the maximum length $r_{\max}$, and we sort the paths according this length, then we can write $(r_{\max} - r)/cK \equiv \Delta T$ which is the constant step between the traveltimes T_k of the sorted paths. Multiplying and dividing the right side of (23) by this step we have

$$\tilde{g}^{\text{3-D}}_{\mathrm{PS,H}} = \lim_{K\to\infty} \frac{A}{c} \frac{cK}{r_{\max} - r} \sum_{k=1}^{K} \delta'(t - T_k)\Delta T. \tag{24}$$

We can convert the sum in (24) to an integral over time by taking the limits $K \to \infty$, $T_k \to T$, and $\Delta T \to dT$, which gives

$$\tilde{g}^{\text{3-D}}_{\mathrm{PS,H}} = A \frac{K}{r_{\max} - r} \int_{r/c}^{r_{\max}/c} \delta'(t - T) dT. \tag{25}$$

We can immediately evaluate the integral in (25) to obtain

$$\tilde{g}^{\text{3-D}}_{\mathrm{PS,H}} = A \frac{K}{r_{\max} - r} [\delta(t - r/c) - \delta(t - r_{\max}/c)]. \tag{26}$$

If now we choose

$$A = \frac{r_{\max} - r}{Kr}, \tag{27}$$

then (26) reduces to

$$\tilde{g}^{\text{3-D}}_{\mathrm{PS,H}} = \frac{\delta(t - r/c)}{r} - \frac{\delta(t - r_{\max}/c)}{r}. \tag{28}$$

The first term on the right side of (28) is the desired Green's function (22), while the second term is an 'artefact' Green's function due to fictituous sources at a distance $r_{\max}$ from the observation point. We can easily identify and ignore the contribution to the waveform from this 'artefact' Green's function is we choose $r_{\max}/c \gg r/c$. Thus the substitution of the term A as defined in (27) for the term $1/N^{p_k}$ in the sum (20) gives a practical path-summation formula which produces the expected Green's function for a constant-velocity medium.

We noted earlier that the path geometry and the normalization term $1/N^{p_k}$ in the sum (20) are independent of the velocity variation. Thus, it is reasonable to apply the rule for path selection and the normalization (27) obtained above for the constant-velocity medium to the case of a smooth, heterogeneous media. Then, substituting (27) for the term $1/N^{p_k}$ in the sum (20), we obtain our final path-summation approximation to the 3-D Green's function response:

$$\tilde{g}^{\text{3-D}}_{\mathrm{PS}}(\mathbf{r}, t; \mathbf{r}_0, t_0 = 0) \approx \lim_{K\to\infty} \frac{r_{\max} - r}{\sqrt{c(\mathbf{r}_0)c(\mathbf{r})}K} \sum_{k=1}^{K} \frac{\delta'(t - T_k)}{r}, \tag{29}$$

where T_k is given by (21). We recall that our choice of normalization requires that the path lengths be distributed uniformly between the source to observation-point distance r and the maximum path length $r_{\max}$ used in the sum.

To arrive at (29) we followed a heuristic development where we assumed but did not demonstrate the convergence of the infinite sum (5), and we made several strong approximations following from the smoothness of the medium. In particular, the choice of Green's function (13) and (14) and the simplification from (18) to (19) explicitly neglects local, multiple scattering; thus the path-summation solutions (20) and (29) locally include only forward propagation.

Two-dimensional path-summation formulation

Although the path-summation approach is intended primarily for 3-D problems, we will require later a 2-D formula for a numerical example comparing path-summation and finite-difference waveforms. We will thus construct an approximate, 2-D analogue to expression (29) which reproduces the correct Green's function response for the homogeneous case. We first write (29) as

$$\tilde{g}_{\mathrm{PS}}^{3\text{-D}} \approx \lim_{K\to\infty} \frac{r_{\max}-r}{\sqrt{c(\mathbf{r}_0)c(\mathbf{r})K}} \sum_{k=1}^{K} -\frac{\partial}{\partial T}\frac{\delta(t-T)}{r}\bigg|_{T=T_k}. \tag{30}$$

This expression shows that the path-summation formula (29) is an algorithm that sums time derivatives of the Green's function, shifted in time according to the traveltime $T_k = r_k/c$ along each path. We will construct the equivalent algorithm using the 2-D Green's function for an impulsive source (Morse & Feshbach 1953; Tolstoy 1973)

$$g_{\mathrm{H}}^{2\text{-D}}(\mathbf{r}, t; \mathbf{r}_0, 0) = \frac{2h(t-T)}{\sqrt{t^2-T^2}}, \tag{31}$$

where $r = \|\mathbf{r}-\mathbf{r}_0\|$, $T = r/c$, and $h(x)$ is the Heaviside unit step-function. Forming a sum analogous to (29) by taking the derivative with respect to traveltime T of (31) and then evaluating the result at the traveltime T_k along each path, we form a 2-D path-summation formula,

$$\tilde{g}_{\mathrm{PS}}^{2\text{-D}}(\mathbf{r}, t; \mathbf{r}_0, t_0 = 0) \approx \lim_{K\to\infty} \frac{r_{\max}-r}{\sqrt{c(\mathbf{r}_0)c(\mathbf{r})K}} \sum_{k=1}^{K} -\frac{\partial}{\partial T}\frac{2h(t-T)}{\sqrt{t^2-T^2}}\bigg|_{T=T_k}. \tag{32}$$

It can be easily shown that this formula reproduces the correct Green's function for the homogeneous case by following the steps used above to convert the path sum to an integral for the 3-D case.

For computational efficiency, we will use a modified form of the 2-D path-summation formula (32) for the 2-D example below. We simplify (32) by replacing the evaluation *within the path sum* of the Green's function for traveltime T_k along each path with a single convolution *after the path sum* with the homogeneous-medium Green's function $2h(t-r/\bar{c})/\sqrt{t^2-(r/\bar{c})^2}$, where $\bar{c}$ is the mean velocity along the fastest path in the sum. Thus we arrive at the 2-D path-summation formula

$$\tilde{g}_{\mathrm{PS}}^{2\text{-D}}(\mathbf{r}, t; \mathbf{r}_0, t_0 = 0) \approx \lim_{K\to\infty} \frac{r_{\max}-r}{\sqrt{c(\mathbf{r}_0)c(\mathbf{r})K}} \frac{2h(t-r/\bar{c})}{\sqrt{t^2-(r/\bar{c})^2}} \otimes \sum_{k=1}^{K} \delta'(t-T_k), \tag{33}$$

where $\otimes$ is the convolution operator.

Path-summation formulation for arbitrary source time functions

The discrete, path-summation formulation for the response $\psi(\mathbf{r}, t)$ at observation location $\mathbf{r}$ for a point source $q_0(\mathbf{r}_0, t)$ in a heterogeneous medium with velocity distribution $c(\mathbf{r})$ is given by the convolution of the source time function with the path-summation 'Green's' function $\tilde{g}_{\mathrm{PS}}$; that is,

$$\psi(\mathbf{r}, t|\mathbf{r}_0, t_0) = q_0(t) \otimes \tilde{g}_{\mathrm{PS}}(\mathbf{r}, t|\mathbf{r}_0, t_0). \tag{34}$$

The path-summation 'Green's' function $\tilde{g}_{\mathrm{PS}}$ is given by (29) in three dimensions, and by (32) or approximately by (33) in two dimensions. The traveltime T_k is given by the integral over slowness along each path,

$$T_k = \int_{\mathbf{r}_0}^{\mathbf{r}} \frac{ds_k}{c(\mathbf{r})}, \tag{35}$$

where we define a parametric path s_k and an increment ds_k along this path by

$$s_k \equiv \mathbf{x}(p); \quad 0 \le p \le 1; \quad \mathbf{x}(0) = \mathbf{r}_0, \quad \mathbf{x}(1) = \mathbf{r}, \qquad ds_k = \sqrt{\sum_{i=1}^{D} dx_i^2}, \tag{36}$$

where p is a parameter and D is the spatial dimension of the problem.

Practical application of the path-summation formulas to a scalar wave equation problem requires a summation over a finite number of paths (i.e. K finite) between the source and the observation point $\mathbf{r}$; this gives a waveform solution $\psi(\mathbf{r}, t)$ for the problem that is an approximation to the finite-frequency response with appropriate amplitude scaling. Note, however, that since we evaluate the path summation using a finite, Monte Carlo summation, the 'Green's' function waveform we obtain will be in general very 'spiky' and so may not be useful in practice before convolution with a smooth source time function.

Discussion of the path-summation formulation

Some discussion of the path-summation formula and its justification is useful to illuminate the character, range of validity and limitations of the method. First, note that we have obtained a path-summation solution for the scalar wave equation using a traveltime—the integral of slowness along a spatial path. This approach differs from the use in the Feynman path-integral method of the classical action, the integral of the Lagrangian along a space–time path. While the action integral in the Feynman path-integral method is related to the principle of least (stationary) action, the integral over slowness in our formulation is related to Fermat's principle of least (stationary) time. Our path-summation solution produces a waveform—a time-varying amplitude, instead of a single amplitude value related to the probability for the state of a quantum particle obtained with the Feynman path integral.

Second, because the integral over slowness in (35) is independent of integration direction along the path, the path-summation formulation is symmetric for an exchange of the source and observation points. Consequently, the path-summation formula follows the principle of reciprocity (e.g. Morse & Feshbach 1953).

Third, recall that we made no assumptions about the frequency content of the source. In practical applications of the method, however, the necessity of using a finite number of paths gives a corresponding coarse sampling of the medium. Consequently, the resulting waveform will only form a useful approximation of the complete solution up to some highest frequency or corresponding shortest wavelength. This wavelength depends on the number of paths sampled, the roughness of the medium and the distance between the source and observation points.

Finally, note that the conditions we imposed on the path geometry to obtain normalization terms for the practical path-summation formula do not depend on the velocity distribution $c(\mathbf{r})$. Thus we always construct a geometrically 'uniform' representative sample of paths, regardless of the velocity distribution. The signal on the waveform for a heterogeneous medium differs from that for a homogeneous medium because of the non-uniform distribution of traveltimes produced in a heterogeneous medium by the geometrically 'uniform' set of paths. This asymmetry between the path geometry and the traveltimes gives imperfect cancellation of the elementary signals and so produces features on the waveform.

APPLICATION OF THE PATH-SUMMATION METHOD

The practical implementation of the path-summation method has two main components: (1) the specification and selection of a representative set of paths; and (2) the construction of a waveform using the elementary signals contributed by each path.

Recall that in developing the path-summation formulation we required that:

(1) the velocity distribution $c(\mathbf{r})$ is smooth;

(2) the maximum path length $r_{\max}$ is sufficiently greater than the distance r from the source to the observation point that the truncation of the path summation and the corresponding artefact signal occurs at a time $T_{\max}$ later than any time of interest;

(3) the path lengths are uniformly distributed between the minimum and maximum lengths r and $r_{\max}$.

Path specification and selection

A 'well-distributed' sample of 'all possible paths' is necessary for the accurate, rapid convergence of the path-summation method. Consequently, the specification of the geometry and distribution of the paths and the selection of methods to construct these paths efficiently are primary concerns in the application of this method. We require a finite set of paths that samples the medium in the same way and gathers the same information as the infinite set of 'all possible paths', and which satisfies the conditions set above in the justification of the path-summation formula. Since we can only work with a relatively small sample of paths, it is reasonable to restrict our selection to the 'least exceptional' paths, that is smooth paths with few inflection points. This choice may be adequate for smooth media, such as in our 2-D example below, but will prevent the inclusion of multiple-scattering effects in velocity models with sharp boundaries or strong gradients. We will assume that the path geometry need only allow a radius of curvature of the paths of the order of and larger than the characteristic wavelength corresponding to the dominant period T_0 of the source.

To meet these requirements, we specify the paths in the present work using cubic B-splines. A cubic B-spline (Fig. 3) is a smooth, parametric curve whose shape and location is controlled by a set of control vertices (e.g. Bartels *et al.* 1987). For the path-summation application we use a spline formulation with special end conditions (Michelini 1995) so that the paths connect to the first and last control vertices (i.e. the source and observation points). We use three to seven vertices, including the source and observations points, in the examples presented below. The main difficulty encountered with this method of path specification is in obtaining a uniform distribution of path lengths because of the complicated relationship between the location of the control vertices and the location of the resulting path.

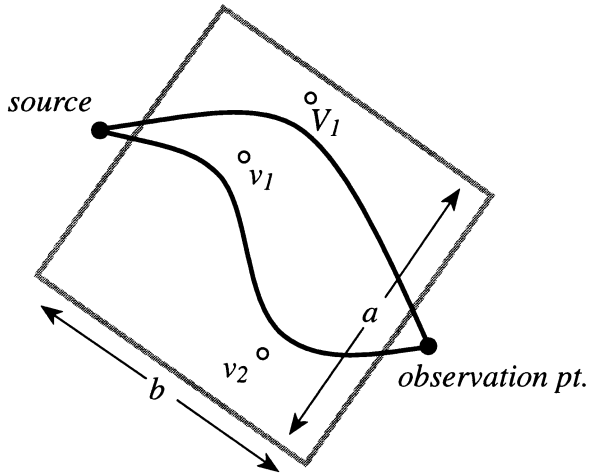

Figure 3. Examples of cubic B-spline paths. The locations of the control vertices v_1 and v_2 for a two-vertex path or V_1 for a single-vertex path are selected at random within a pre-defined region $a \times b$ (thick grey lines); this region may include the source and receiver if back-scattering is desired. The spline path is a smooth curve between the source and observation points that passes near, but not through, the intermediate control vertices.

Additionally, each path is subject to two tests before application of the computationally expensive slowness integral along the path. First, the path is rejected if its length is greater than the pre-determined, maximum length $r_{\max}$. Second, for problems where the model is only specified within a limited region, a path is rejected if any part of it falls outside this region.

Waveform construction

In practical applications, the waveform representing the response at an observation point is constructed following the path-summation formula (34) using a discrete time series $\psi(t_i)$. For each path that is sampled, the discrete equivalent of the derivative of a Dirac delta function is summed into the time series $\psi(t_i)$ at the time t_i closest to the time $t = t_0 + \int_{\mathbf{r}_0}^{\mathbf{r}} ds_k/c(\mathbf{r})$, the source reference time t_0 plus the traveltime for the path obtained by numerical integration of slowness along the path. When all paths have been sampled, the time series $\psi(t_i)$ is convolved with the source time function and scaled by the factor $(r_{\max} - r)/\sqrt{c(\mathbf{r}_0)c(\mathbf{r})}K$. In addition, because it is difficult in practice to obtain a uniform distribution of path lengths, the contribution from each path is scaled in amplitude to produce the equivalent of a uniform distribution of lengths. This amplitude scaling α for a path of length L is inversely proportional to the number of paths K_L with length between L and $L + \Delta L$; that is, $\alpha = K/K_L$ where K is the total number of paths sampled. No corrections for focusing, defocusing or other non-dissipative amplitude changes due to changes in the medium velocity along the individual path are applied—these effects are accounted for in the summation over paths

through the constructive and destructive interference of the contributions to the waveform for each path.

Finally, the time series is multiplied by $1/r$ for a 3-D simulation, or convolved with $2h(t-r/\bar{c})/\sqrt{t^2-(r/\bar{c})^2}$ in two dimensions, where $\bar{c}$ is the mean velocity of the medium. Note that the 3-D construction reproduces exactly the corresponding path-summation 'Green's' function (29), but, as noted earlier, the 2-D construction uses an approximation to the formula (32) for efficiency. That is, the convolution with $2h(t-r/\bar{c})/\sqrt{t^2-(r/\bar{c})^2}$ after the path summation is a convolution with a homogeneous Green's function using the constants $r/\bar{c}$ for the traveltime and r for the distance. To match (32) exactly, there should be, for each sampled path, a convolution with a 2-D Green's function based on the traveltime T_k and length r_k for the path.

NUMERICAL EXAMPLES

We next examine the performance and behaviour of the path-summation method in three and two dimensions and compare the resulting waveforms with those obtained with accurate existing methods. In the following discussions we use quotes to delimit terms such as 'refracted', 'reflected' and 'diffracted' since these are infinite-frequency and geometrical-ray concepts; they are often not separable as distinct, independent wave phenomena for finite-frequency wavefields.

Low-velocity sphere in three dimensions

We first apply the path-summation method in a 3-D problem consisting of a low-velocity spherical inclusion in a homogeneous whole-space. Strictly, this structure violates our restriction to a smooth medium, but it allows a comparison of the path-summation waveforms with those obtained with an exact analytic solution.

For the 3-D geometry we take a point source in a homogeneous whole-space background with velocity $c = 5\ \mathrm{km\ s^{-1}}$ (Fig. 4). A spherical inclusion of radius 4 km and velocity $3\ \mathrm{km\ s^{-1}}$ is centred at a distance of 20 km from the source. We consider 25 observation locations along a radius normal to the axis through the source point and the centre of the sphere, and the radius intersects this axis at distance of 20 km from the sphere. For this geometry, there is a 'geometrical shadow' region for the observations within 8 km of the axis. This region is illuminated by finite-frequency 'diffracted' waves that can be considered as having passed around the boundary of the sphere; these waves are not produced with infinite-frequency, geometrical-ray theory.

We obtain the exact finite-frequency waveforms from this problem using an analytic method (Korneev & Johnson 1992). This wavenumber-domain method matches boundary conditions across the surface of the sphere to obtain the complete 3-D response due to elastic wave propagation from a point source. We obtain a solution for the scalar wave equation by setting the viscosity equal to zero in the spherical inclusion and near to zero in the whole-space, and using an isotropic pressure source.

We construct path-summation waveforms using the 3-D path-summation formula (34 and 29). However, because of the simplicity and high degree of symmetry of the inclusion and problem geometry, a very small portion of the model, namely the boundary and interior of the sphere, will be

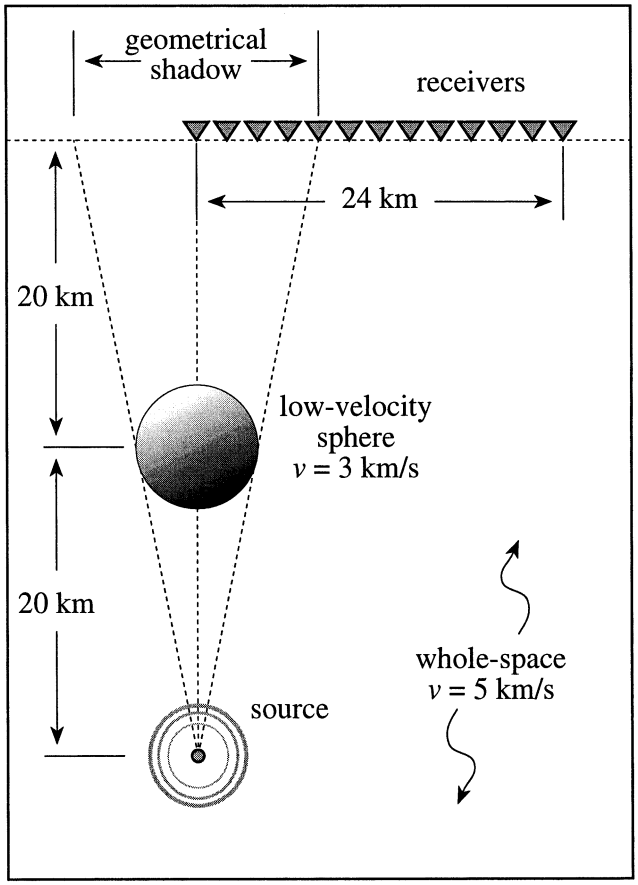

Figure 4. 3-D model geometry and waveform locations. The geometrical shadow region is illuminated by first-arriving 'diffracted' waves, but there are no corresponding geometrical rays.

responsible for differences of the wavefield from that for a homogeneous whole-space. This presents some difficulty for the path-summation method since it is a stochastic, Monte Carlo sampling technique and thus converges most rapidly when features well distributed in the sampled region make important contributions to the solution. Consequently, we apply a basic, non-adaptive 'importance-sampling' in the path selection by using only three or four control vertices, the source and observation locations and one or two points between, to define the cubic B-splines. In this way, we construct paths of the 'class' type that is most likely to contribute to the differences from the homogeneous problem, namely paths that bend only once. We thus are primarily sampling paths that are smooth versions of 'single-scattering' paths; that is, paths composed of one straight segment between the source and a 'scattering' point, and a second straight segment between this 'scattering' point and the observation location. [Sneider & Lomax (1996) have show that a summation over such 'single-scattering' paths recovers the main variations in amplitude and phase of the first-arriving signal in a pseudo-random medium.] This importance sampling improves significantly the recovery on the path-summation waveforms of features seen on the exact waveforms.

Each path-summation waveform consists of a sum over 10 000 paths, which takes only a few seconds of CPU time on a desktop workstation (Hewlett-Packard 715-100 workstation).

For this simulation, if the sum is extended beyond 10 000 paths the background oscillations on the traces are reduced in amplitude, but the shapes of the primary signals on the waveforms do not change appreciably. We use the same source time function for both solution methods.

Fig. 5 shows the exact and path-summation waveforms for the low-velocity spherical inclusion. We find a near-exact agreement for the 'direct' first-arriving pulse at locations beyond 17 km. This result is expected since the wavefield in these regions is not strongly influenced by the sphere, but it also indicates that the path-summation method converges accurately for a 3-D whole-space. There are small mismatches in phase and amplitude between the two methods for the first-arriving pulse at locations less than 16 km. However, the path-summation synthetics reproduce well the general shape and variation of the exact waveforms. Most notably, the path-summation waveforms include the 'diffracted' first-arriving signal in the geometrical shadow zone at distances of 0 to 8 km. This is a finite-frequency wave phenomenon that cannot be recovered with ray theory.

The secondary arrival at about 9 s traveltime on the trace at location 0 km is formed by waves that are 'scattered', 'refracted' and 'focused' by the low-velocity inclusion. Here we also find that the path-summation waveforms show some phase and amplitude differences from the exact results, but again reproduce well the main features of the exact waveforms. In particular, it is notable that the path-summation waveforms reproduce much of the phase shift of this signal relative to the phases of the 'direct' and 'diffracted' signals and the source time function (cf. Fig. 5). This result indicates that the path-summation method can accurately reproduce phase shifts, which are of primary importance in determining the shape of waveforms.

The timing of the 'direct' and 'diffracted' first-arriving signals on the waveforms follows closely the traveltime curve for geometric rays in the absence of the low-velocity spherical inclusion (Fig. 5). This illustrates why traveltime inversion using first-arrival times cannot detect features similar to this low-velocity sphere (Wielandt 1987). The 'information' in the wavefield about the low-velocity sphere is contained primarily in the secondary 'scattered' and 'refracted' signals, and to a lesser degree in the reduced amplitude and slight time delay of the first-arriving 'diffracted' signal in the 'geometrical shadow' region. The path-summation method recovers all of these waveform features; consequently, the use of the path-summation method in a waveform inversion may give more accurate imaging than ray-based first-arrival-time techniques.

Although not perfect, the results of this 3-D simulation are significant because the stochastic path-summation method (with simple importance sampling) performs well for this highly symmetric geometry which has a velocity variation that is not smooth. However, it will be necessary to perform a comparison of the path-summation method with near-exact results for more complicated 3-D structures which are more representative of natural structures and thus of primary interest in inversion problems. Below we present such a comparison for a 2-D problem.

Quasi-random two-dimensional medium

We examine the behaviour of the path-summation method in a complicated, smooth 2-D medium that is representative of the models that might be obtained from inversion of realistic earth structures. We compare the resulting waveforms with those from a finite-difference solution for the scalar wave equation, and we examine the relationship between features of the medium, features on the waveforms, and the corresponding path-summation paths.

Fig. 6 shows the 2-D model and the source and observation locations. The velocity distribution is quasi-random (Gaussian) and strongly varying, with significant features on the scale of and larger than the dominant wavelength of the source. The velocity varies in the range 4.0 ± 1.0 km s^{-1} (± 25 per cent), with an RMS variation of about 0.3 km s^{-1}. A similar model is used in Snieder & Lomax (1996) and Lomax & Snieder (1996) to examine 'single-scattering' and 'wavelength-averaging' techniques for modelling finite-frequency wavefields in complicated structures.

We consider a wide-band point source with centre period $T_0 = 50$ s; this corresponds to a dominant wavelength $\lambda_0 = 200$ km for the mean velocity of the medium, 4.0 km s^{-1}. The observation points are located along a line at distances of about five to eight times the dominant wavelength λ_0. (The physical units we use here are appropriate for the study of, for example, seismic surface-wave propagation. However, these simulations are relevant to other problems with equivalent spatial and time scales when measured in terms of the dominant wavelength and period, respectively, of the source.)

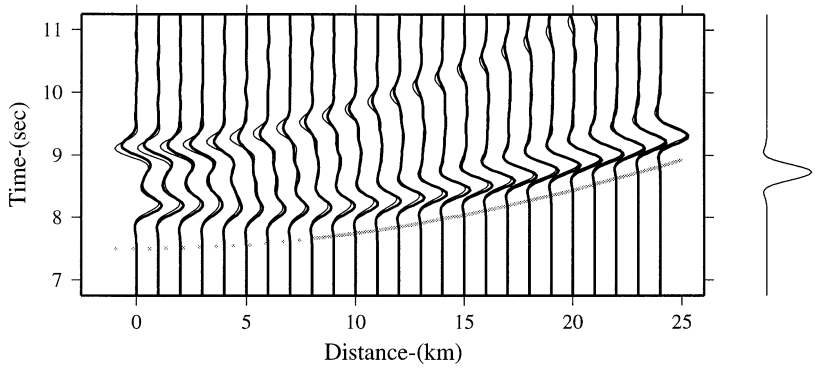

Figure 5. Exact analytic (thin solid lines) and path-summation (thick solid lines) waveforms for the 3-D geometry shown in Fig. 4. The geometrical-ray traveltime curve for the background medium ($c = 5$ km s^{-1}) is shown for outside (thick grey line, distance >8 km) and inside (thick dotted grey line, distance <8 km) the 'geometrical shadow'; this curve is shifted ahead 0.5 s so that it does not overlap the waveforms.

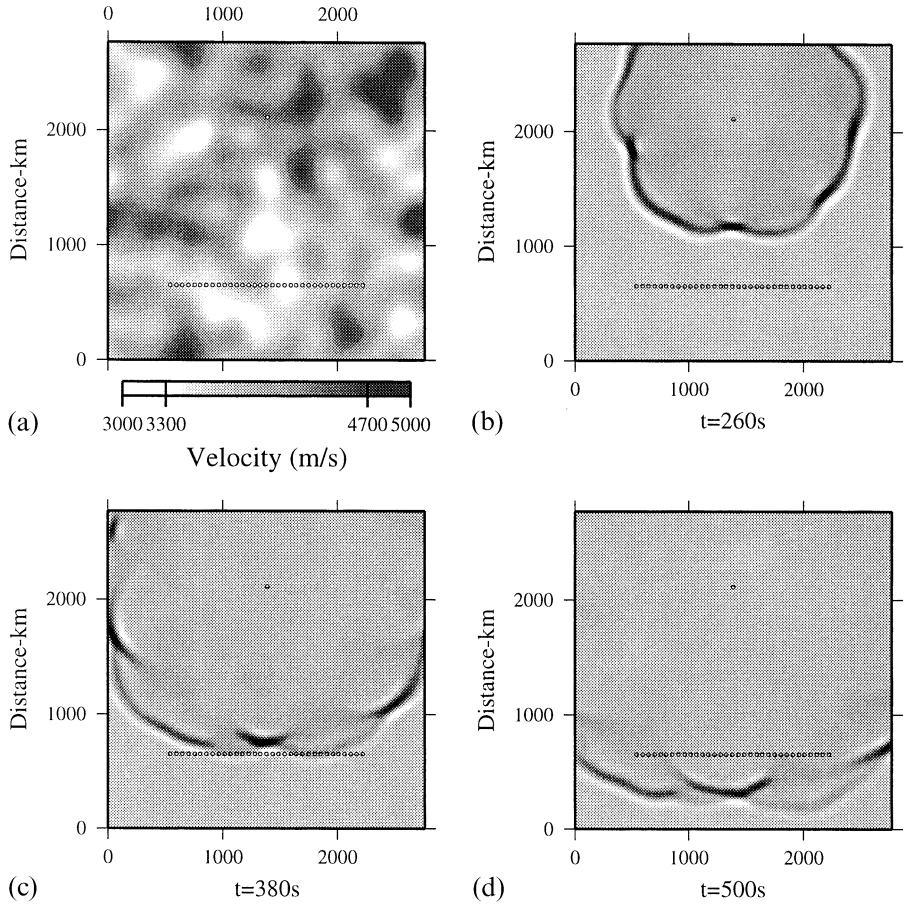

Figure 6. 2-D, quasi-random velocity model. (a) velocity distribution. (b)–(d) 'snapshots' of the FD wavefield at several time instants.

To obtain a near-exact solution to this problem, we use a finite-different (FD) algorithm to solve the scalar wave equation (1) on a 2-D grid. This algorithm is second order in time and fourth order in space, and uses transmitting boundary conditions.

The FD wavefield at several time instants is shown in Fig. 6. As it spreads away from the source, the primary near-circular wavefront breaks into segments that are delayed or advanced, and focused or de-focused as they interact with features of the model. As it passes the line of observation locations, the wavefield is complicated: it consists of several segments formed by interfering 'refracted' and 'diffracted' signals that produce a large range of amplitudes. The first-arriving, low-amplitude signals at observation points located between about 900 to 1300 km and about 1500 to 1900 km are due in part to 'diffracted' waves that have passed around the strong, low-velocity region near the centre of the model. This low-velocity feature also causes a strong focusing of the wavefield that produces the high-amplitude secondary arrivals at observation locations between about 1100 and 1500 km. However, the overall wavefield is not strongly segmented and scattered, and thus it is representative of signals with maximal information content for the purpose of deterministic waveform inversion to infer velocity structure.

We construct path-summation waveforms using the approximation to the 2-D path-summation formula (34 and 33) for the same observation locations, source location and source time function as in the FD simulation. Each path-summation waveform consists of a sum over 10 000 paths and requires a few seconds calculation time on our desktop workstation. This time is about 1/1000th of the CPU time needed for the entire FD calculation, although a single FD calculation can produce waveforms at any or all grid nodes. The FD and path-summation waveforms for this 2-D simulation are shown in the lower part of Fig. 7. Fig. 8 shows the spatial distribution of all paths used to construct a waveform, the paths that contribute to the first-arriving signal for the case of a homogeneous model, and the paths that contribute to significant signals on several of the waveforms for the quasi-random media.

The prominent signal beginning at about 550 s on all of the path-summation traces is due to the truncation of the summation for paths lengths $r_k \geq r_{\max}$; this artefact can be easily identified and ignored during application of the method. For times earlier than this artefact, all the path-summation traces show a close resemblance to the corresponding FD traces.

Note that this resemblance includes places where there is no 'signal' on the FD waveforms. This is important since with the path-summation method there are contributions to the waveform at all times between the first arrival and the cut-off due to $r_{\max}$; these contributions must interfere properly to sum to a near-zero trace. In effect, all of the waveform represents a 'response' to a significant volume of the medium with both the FD and path-summation methods. In contrast, ray methods produce only a few signals on the waveform, and these signals represent information only from a few lines or thin tubes in the medium.

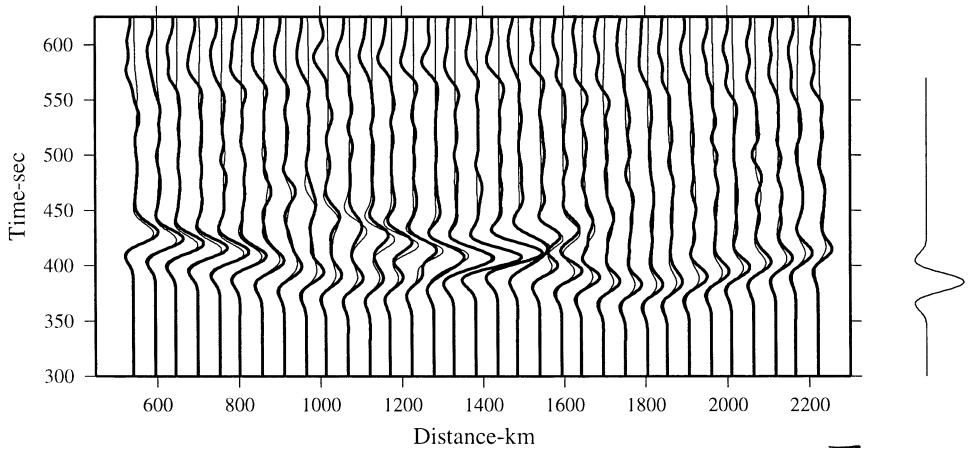

Figure 7. FD (thin lines) and path-summation (thick lines) waveforms for the 2-D quasi-random model shown in Fig. 6.

There is good agreement in both amplitude and phase between the FD and path-summation waveforms for most parts of the waveforms. In particular, the path-summation waveforms show excellent recovery of the significant changes in signal amplitude, phase and timing in the region of focusing and interference around 1400 km. The cause of this change in the signal and an explanation for the accuracy of the path-summation results can be understood by considering the paths that contribute to this signal for observation location 1327 (Fig. 8c). There are a large number of paths that fill a relatively large subvolume of the model relative to the volume filled by the first-arriving paths for the homogeneous case (Fig. 8b). The paths for the quasi-random model are 'focused' by the central low-velocity region; that is, paths with a variety of lengths and positions give similar traveltimes, and so interfere constructively to form the high-amplitude signal. It is also interesting to note in Fig. 8(c) that the paths that contribute most to the high-amplitude signal pass to either side of the low-velocity region and avoid the shorter route through the middle of this region. These paths thus indicate the existence of at least two, stationary-time, 'Fermat' paths for this signal. This phenomenon is recovered well by the path-summation method but would lead to significant difficulty for inversion using geometrical-ray modelling or ray-bending algorithms.

In contrast to this excellent signal recovery in a region of focusing, the path-summaton waveforms show an overestimate of amplitude for the early first-arriving signals on the waveforms for locations around 1100 and 1700 km. An examination of the paths that contribute to the signal at locations 1067 km (Fig. 8e) and 1695 km (Fig. 8d) shows that they fill a small volume that has an arcuate form. This volume is related to the minimum-time, 'Fermat' path between the source and observation points. It may be that the mismatch in amplitude of this signal is due to a relative undersampling in the path construction algorithm of paths similar to the 'Fermat' path.

The path-summation synthetics recover well a significant 'secondary' signal at about 425 s and later on the waveforms for locations between about 900 and 1300 km and between about 1500 and 1700 km. These are 'refracted' and 'diffracted' waves, some of which cannot be produced by ray-based methods. These signals are related to paths that bend through and around the central low-velocity region (e.g. location 1067 km, Fig. 8f). In terms of the path summation, the existence of this signal is caused by an asymmetry in the distribution of paths that contribute to the waveform around the time of these signals. This asymmetry is apparent in Fig. 8(f) in the increased density of paths to the right side of the volume filled by the paths. In contrast, the paths that contribute to the first arrival at location 1067 km pass to the left of the low-velocity region (Fig. 8e)

As with the 3-D low-velocity sphere example, if the path sum is extended beyond 10 000 paths the small background oscillations on the traces are reduced in amplitude, but the shapes of the primary signals on the waveforms do not change appreciably. In particular, the mismatches in phase and amplitude discussed above do not change significantly as the number of paths is increased beyond 10 000. It appears that deficiencies in the path-summation waveforms may be due to inherent limitations of this approximate method, or they may be due to the difficulty of constructing and selecting a 'representative' sample of paths.

For this 2-D simulation, since each path-summation synthetic requires about 1/1000th of the computation time required for the complete FD simulation, the complete set of 33 path-summation waveforms requires about 1/100th of the time of the FD calculation. Consequently, depending on the number of waveforms required, the path-summation method would be from one to three orders of magnitude faster than the equivalent FD simulation. The path-summation calculation also requires insignificant computer memory over that required to store the velocity model. Since it is not necessary with the path-summation method to store the model in a grid, the model can be specified using a compact, analytic or geometrical description. This reduction in memory requirements over finite-difference and finite-element numerical methods may be significant or critical in both two- and three-dimensional applications.

In addition, the path distributions shown in Fig. 8 form a finite-bandwidth, multiple-scattering generalization of the single-frequency, single-scattering 'wavepaths' that have been proposed recently for waveform inversion (e.g. Woodward 1992). Like these 'wavepaths', the sets of path-summation paths and associated traveltimes represent a relationship between time intervals on a waveform and volumes in the model. Such a relationship is required for many waveform inversion methods, and thus there is an indication that the path-summation results could be used for inversion in the framework of these methods.

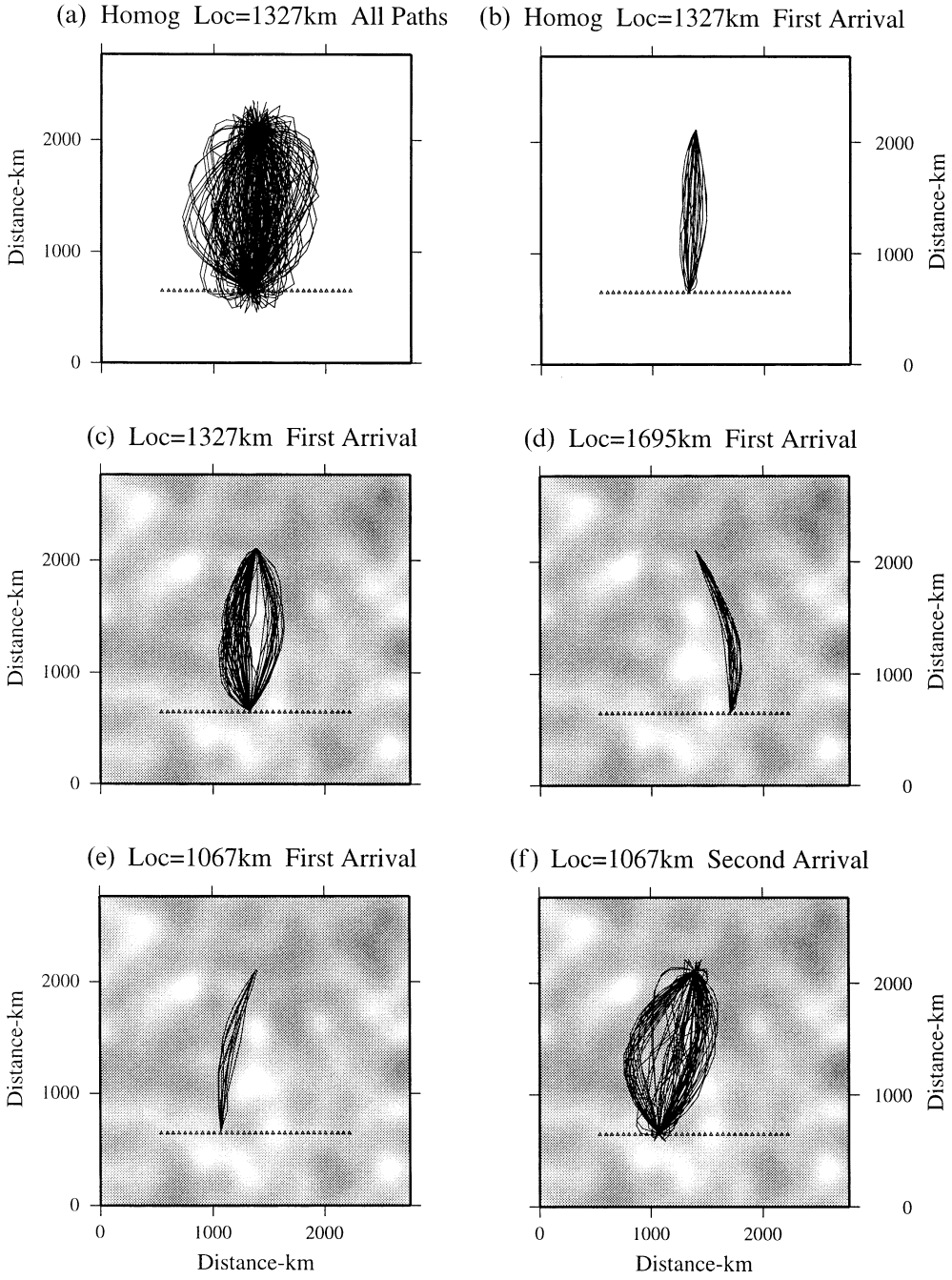

Figure 8. Path-summation paths for selected observation locations for a homogeneous model and for the 2-D, quasi-random model simulation. (a) A uniform sample of all paths used in the path-summation sum; these paths are representative of the distributions of paths for any velocity model or source–receiver pair. (b)–(f) Path samples drawn in proportion to the envelope of the signal to indicate the relationship among 'significant' signals on the waveform, the path geometry and the model. (b) Paths contributing to the first-arriving signal at location 1327 km in a homogeneous model. Samples for the quasi-random model of (c) paths contributing to the main pulse at $t \sim 410$ s at location 1327 km; (d) paths contributing to the main pulse at $t \sim 380$ s at location 1695 km; and paths contributing at location 1067 km to (e) the first pulse at $t \sim 390$ s and (f) the second pulse at $t \sim 450$ s.

The recovery by the path-summation method of all wave types and the overall quality of the match between the two sets of waveforms indicates that the path-summation waveforms are accurate enough to give a meaningful misfit value with observed waveforms. This, combined with the speed of the method, indicates that the path-summation method may make possible stochastic, global, waveform inversion for problems with geometry and scaling similar to that presented in this example.

DISCUSSION

The difference between the path-summation method and other techniques for the synthesis of wave propagation follows from the consideration of a representative sample of 'all possible' paths between the source and observation points in the path-summation method. Ray-based methods sample the medium along a small number of 1-D, Fermay rays, regardless of the

dimension of the medium, while the path-summation method considers a finite subvolume with the same dimension as the medium. The path-summation method includes the interaction of the wavefield with variation of the medium properties throughout this finite volume. Consequently, the resulting waveforms include amplitude variations, 'diffractions' and other full-wave features that are difficult or impossible to obtain with ray methods.

Frequency–wavenumber of modal-summation techniques sum over global, analytic solutions such as plane waves or exponential eigenfunctions; the existence and validity of these solutions is inseparable from symmetry and simplicity in the model geometry. In contrast, the local, direct sampling of the medium in the path-summation method does not make any strong requirements on the model geometry and so allows the consideration of more complicated structures.

Finite-difference and finite-element numerical methods may be thought of as systematically including all possible paths between all nodes on a regular grid. The path-summation method, on the other hand, considers only a sample of the possible paths between the source and observation point, and it requires only simple, rapid, slowness integration along these paths. This difference leads to the significant reduction in calculation time for individual waveforms with the path-summation method relative to numerical methods, but also accounts for the approximate nature of the path-summation results.

Although not examined systematically in this paper, it is apparent that the rate and accuracy of convergence of the path-summation method are dependent on certain parameters of the problem. The convergence time (measured by the number of paths sampled) will increase, in general, as the distance between the source and receiver or the length of the time window required on the waveform is increased; that is, the convergence time increases with the size of the subvolume of the model that is sampled. The convergence time may also increase with decreasing dominant period of the source time function, or as the amplitude of the dominant features in the medium is increased or their characteristic scale-length is reduced. For example, for complicated media with time and spatial scaling similar to the 2-D numerical example examined here, the convergence is rapid when the distance R between the source and the observation point is up to the order of 10 times the dominant wavelength in the source signal. However, as the velocity distribution becomes smoother, the maximum distance R of applicability will increase.

Two of the primary concerns in the application of the path-summation method are the definition and the construction of a set of paths that is representative of all possible paths between a source and observation point. We have not addressed these issues in detail in this paper, although they are likely to be of importance in future development of the method. We may note that the set of paths need only include those that give traveltimes less than the maximum time of interest, and that, from the derivation of the method, the paths must be well distributed in total length and in direction at the source and receiver points. This leaves some freedom in the selection of paths, but it is also likely that some of the shortcomings of our numerical applications of the path-summation method were related to the path geometry. Consequently, it is desirable to obtain a good working definition of appropriate path geometry, although it is not clear that this can be done rigorously, in the mathematical sense.

There is also the possibility that the use of importance sampling in the selection of paths will improve the efficiency of the path-summation method, in analogy to the use of importance sampling in Monte Carlo integration (e.g. Hammersley & Handscomb 1967). For the path-summation summation, importance sampling could be achieved by preferential selection of the paths that contribute to the parts of the waveform that will have the most significant signal after the solution has converged. However, as with all importance sampling, this selection must be done carefully, and the resulting non-uniform sampling must be properly normalized, otherwise spurious signals and amplitude and phase errors will result.

Although there is always some error in the path-summation waveforms due to the stochastic nature of the path sum, this method exhibits a great increase in computational efficiency over finite-difference, finite-element and boundary integral methods. Moreover, in many cases errors in the waveforms will not be significant relative to other sources of error such as noise in the data, or simplifications in the model parametrization. Also, the set of sampled paths and associated traveltimes produced by the path-summation method give information about the relationship between features in the waveform and in the model. This type of information is required for iterative, directed inversion methods, but it is difficult or impossible to obtain from the results of numerical modelling with finite differences of finite elements.

CONCLUSIONS

We have presented a heuristic development and applications of a Monte Carlo path-summation method to obtain approximate waveform solutions to the scalar wave equation for a smooth, heterogeneous medium.

Because it is a numerical, stochastic method, the convergence rate of the path-summation method depends on the source–receiver distance, the medium properties and the dominant wavelength of the source. Our applications of the path-summation method indicate that it can produce rapidly the main features of the early arriving, finite-frequency wavefield in complicated 2-D and 3-D structures.

The speed and accuracy of the method may be sufficient to allow waveform inversion in three dimensions; this is significant for analysis of acoustic and elastic waveforms in natural sciences such as seismology and ocean acoustics where complicated, irregular distributions in material properties are expected.

ACKNOWLEDGMENTS

I thank Jean Virieux for discussions and suggestions that helped to shape the theoretical part of this work. The path-summation method follows from inspiring work I did with Roel Snieder. The critical and helpful comments of Brian Schlottmann, Guust Nolet and two anonymous reviewers added much to the manuscript. I thank Valeri Korneev for providing the analytic, 3-D, spherical inclusion waveforms and Henk Marquering for the 2-D finite-difference code. I did part of this research while a visiting researcher at ICTP, Trieste, Italy; I am most grateful to Alberto and Luisa Michelini for their unfailing support, interest and hospitality during my stay in Trieste.

REFERENCES

Bartels, R.H., Beatty, J.C. & Barsky, B.A., 1987. *An Introduction to Splines for use in Computer Graphics and Geometric Modelling,* Morgan Kaufmann, Los Altos, CA.

Born, M. & Wolf, E., 1964. *Principles of Optics,* Pergamon Press, Oxford.

Carter, J.A. & Frazer, L.N., 1984. Accommodating lateral velocity changes in Kirchhoff migration by means of Fermat's principle, *Geophysics,* **49,** 46–53.

Dashen, R., 1979. Path integrals for waves in random media, *J. math. Phys.,* **20,** 894–920.

Feynmann, R.P., 1948. Space-time approach to non-relativistic quantum mechanics, *Rev. Mod. Phys.*, **20,** 367–387.

Feynman, R.P., 1985. *QED: The Strange Theory of Light and Matter,* Princeton University Press, Princeton.

Feynman, R.P. & Hibbs, A.R., 1965. *Quantum Mechanics and Path Integrals,* McGraw-Hill, New York.

Fishman, L. & McCoy, J., 1983. Derivation and application of extended parabolic wave theories. II. Path integral representations, *J. math. Phys.,* **25,** 297–308.

Frazer, L.N. & Sinton, J.B., 1984. A Kirchhoff method for the computation of finite-frequency body wave synthetic seismograms in laterally inhomogeneous media, *Geophys. J. R. astr. Soc.,* **78,** 413–429.

Hammersley, J.M. & Handscomb, D.C., 1967. *Monte Carlo Methods,* Methuen, London.

Khandekar, D.C., Lawande, S.V. & Bhagwat, K.V., 1993. *Path-integral methods and their applications,* World Scientific, Singapore.

Klauder, J.R., 1986. Path integrals and Semiclassical approximations to wave equations, in *Path Integrals from meV to MeV,* eds Gutzwiller, M., Inomata, A., Klauder, J. & Streit, L., World Scientific, Singapore.

Korneev, V.A. & Johnson, L.R., 1992. Scattering of elastic waves by a spherical inclusion—1. Theory and numerical results, *Geophys. J. Int.,* **115,** 230–250.

Lomax, A. & Sneider, R., 1996. Estimation of finite-frequency waveforms through wavelength dependent averaging of velocity, *Geophys. J. Int.,* **126,** 369–381.

Michelini, A., 1995. An adaptive-grid formalism for traveltime tomography, *Geophys. J. Int.,* **121,** 489–510.

Morse, P.M. & Feshbach, H., 1953. *Methods of Theoretical Physics,* McGraw-Hill, New York.

Patton, R.S., 1986. Ocean acoustics and path integrals, in *Path Integrals from meV to MeV,* eds Gutzwiller, M., Inomata, A., Klauder, J. & Streit, L., World Scientific, Singapore.

Samelsohn, G. & Mazar, R., 1996. Path-integral analysis of scalar wave propagation in multiple-scattering random media, *Phys. Rev. E,* **54,** 5697–5706.

Schlottmann, B., 1999. A path integral formulation of acoustic wave propagation, *Geophys. J. Int.,* **137,** 353–363.

Schulman, L.S., 1981. *Techniques and Applications of Path Integration,* Wiley, New York.

Schulman, L.S., 1988. Introduction to the path integral, in *Path Summation: Achievements and Goals,* eds Lundqvist, S., Ranfagni, A., Sa-yakanit, V. & Schulman, L., World Scientific, Singapore.

Scott, P. & Helmberger, D., 1983. Applications of the Kirchhoff–Helmholtz integral to problems in seismology, *Geophys. J. R. astr. Soc.,* **72,** 237–254.

Snieder, R. & Lomax, A., 1996. Wavefield smoothing and the effect of rough velocity perturbations on arrival times and amplitudes, *Geophys. J. Int.,* **125,** 796–812.

Tolstoy, I., 1973. *Wave Propagation,* McGraw-Hill, New York.

Wiegel, F.W., 1986. *Introduction to Path-Integral Methods in Physics and Polymer Science,* World Scientific, Singapore.

Wielandt, E., 1987. On the validity of the ray approximation for intepreting delay times, in *Seismic Tomography,* pp. 85–98, ed. Nolet, G., Reidel, Dordrecht.

Wielandt, E., 1993. Propagation and structural interpretation of non-plane waves, *Geophys. J. Int.,* **113,** 45–53.

Williamson, I.P., 1975. The broadening of pulses due to multipath propagation of radiation, *Proc. R. Soc. Lond.,* A., **342,** 131–147.

Woodward, M.J., 1992. Wave-equation tomography, *Geophysics,* **57,** 15–26.

Ziolkowski, R.W., 1986. A path-integral-Riemann-space approach to the electromagnetic wedge diffraction problem, *J. math. Phys.,* **27,** 2271–2281.